

Improvement on a Masked White-box Cryptographic Implementation

Seungkwang Lee and Myungchul Kim

Information Security Research Division, ETRI
skwang@etri.re.kr

Abstract. White-box cryptography is a software technique to protect secret keys from attackers who have access to memory for cryptographic algorithms. By adapting techniques of differential power analysis to computation traces containing runtime information such as memory accesses of the target software, Differential Computation Analysis (DCA) has been recovered the secret keys from white-box cryptographic implementations. In order to thwart DCA, a masked white-box implementation has been suggested. However, each byte of the round output was not masked and just permuted by byte encodings. This is the main reason behind the success of DCA variants on the masked white-box implementation. In this paper, we improve the masked white-box cryptographic implementation in such a way to protect against DCA variants by obfuscating the round output with random masks. Specifically, we implement a white-box AES implementation combined with masking techniques applied to the key-dependent intermediate value and the several outer-round outputs. Our analysis and experimental results show that the proposed method can protect against DCA variants including DCA with a 2-byte key guess, collision and bucketing attacks. This work requires approximately 3.7 times the table size and 0.7 times the number of lookups compared to the previous masked WB-AES implementation.

Keywords: White-box cryptography, DCA, collision attack, bucketing attack, countermeasure.

1 Introduction

One of the most important issues in software implementations of cryptographic algorithms is to protect the secret key from various threats. The implementation technique to protect the key from white-box attackers who can access and modify all resources in the device where the cryptographic algorithm runs is called white-box cryptography. In general, white-box cryptography precomputes a series of lookup tables for all input values for each operation and obfuscates the tables with linear and non-linear transformations (i.e. encoding) to prevent the key from being analyzed [10, 11, 16]. After generating the key-instantiated lookup tables above, actual encryption or decryption operation consists of a series of table lookups that replace most of operations.

It is not possible to extract the key from white-box cryptographic implementations simply by observing the intermediate values in memory. Previously, the key extraction from white-box cryptography was largely dependent on cryptanalysis [4, 14, 19, 23, 24, 27], which requires detailed knowledge of the target implementations. Recent attacks, on the other hand, have adapted techniques of differential power analysis and thus an in-depth understanding of the target implementation is not necessary. In particular, it is possible to conduct power analysis on white-box cryptography [26]. In addition, Differential Computation Analysis (DCA) [7] uses the same statistical technique of power analysis such as Correlation Power Analysis (CPA) [9], but this shows the improved efficiency by using computation traces (also known as software execution traces) consisting of noise-free information such as memory accesses, instead of the noisy power traces.

One of the most well-known techniques protecting against power analysis is masking [1, 5, 12, 22], which randomizes every intermediate values for each execution of encryption. In [17], a masked white-box AES (WB-AES) implementation for protecting DCA is proposed. This uses random masks for each value of the intermediate value and thus eliminates the need to mask the lookup tables every time an encryption operation is performed. However, it has been broken by various variants of DCA. For example, each subbyte of the first round output can be the target by making a 2-byte key guess [25]. A collision-based DCA attack in [25] is also similar to this attack, but the analysis method of computation traces is different. A bucketing attack [28] can be successful with chosen-plaintext sets, in which the plaintexts are divided into two set based on the predefined four bits of a hypothetical round output. Here it is important to notice that these vulnerabilities come from the fact that a masked WB-AES implementation does not apply masking on the round output.

In this paper, we improve a masked WB-AES implementation in such a way to protect against these recently published vulnerabilities. The key point is to apply masking not only to the intermediate values but also to the round outputs computed with less than 128 bits of the key. Our evaluation shows that the proposed method provides protection against DCA-variant attacks and the additional cost is a table size that is 3.7 times larger than the previous masked WB-AES implementation. The rest of the paper is organized as follows. Section 2 briefly explains a masked WB-AES implementation and the Walsh transforms used to evaluate the correlation between the hypothetical value and the encoded lookup value. Section 3 reviews the vulnerabilities to DCA-variant attacks. Section 4 presents our improvement on a masked WB-AES implementation of and Section 5 evaluates its security and performance. Finally, Section 6 concludes this paper.

2 Background

This section provides a brief overview of a masked WB-AES implementation for 128-bit key size and the Walsh transform used in this paper to quantify the correlation between two values.

2.1 Masked WB-AES Implementation

By pushing the initial AddRoundKeys into the first round, the AES-128 algorithm can be expressed as follows, with two round keys involved in the final round:

```

state ← plaintext
for r = 1 ⋯ 9
    ShiftRows(state)
    AddRoundKey(state,  $\hat{k}^{r-1}$ )
    SubBytes(state)
    MixColumns(state)

ShiftRows(state)
AddRoundKey (state,  $\hat{k}^9$ )
SubBytes(state)
AddRoundKey(state,  $k^{10}$ )
ciphertext ← state,

```

where k^r is a 4×4 matrix of round keys in the round r , and \hat{k}^r is the result of applying ShiftRows to k^r . To generate lookup tables for the above algorithms, T -boxes combined with SubBytes and AddRoundKeys are generated as:

$$\begin{aligned}
 T_{i,j}^r(x) &= S(x \oplus \hat{k}_{i,j}^{r-1}), \quad \text{for } i, j \in [0, 3] \text{ and } r \in [1, 9], \\
 T_{i,j}^{10}(x) &= S(x \oplus \hat{k}_{i,j}^9) \oplus k_{i,j}^{10} \text{ for } i, j \in [0, 3],
 \end{aligned}$$

where S implies the AES S-box. From the first to the ninth rounds, column vectors in the MixColumns matrix MC are multiplied with values from T -boxes. Let $[x_0, x_1, x_2, x_3]^T$ be a column vector of the state after mapping the round input to T -boxes. Then we have:

$$\begin{aligned}
 & \begin{bmatrix} 02 & 03 & 01 & 01 \\ 01 & 02 & 03 & 01 \\ 01 & 01 & 02 & 03 \\ 03 & 01 & 01 & 02 \end{bmatrix} \begin{bmatrix} x_0 \\ x_1 \\ x_2 \\ x_3 \end{bmatrix} \\
 &= x_0 \begin{bmatrix} 02 \\ 01 \\ 01 \\ 03 \end{bmatrix} \oplus x_1 \begin{bmatrix} 03 \\ 02 \\ 01 \\ 01 \end{bmatrix} \oplus x_2 \begin{bmatrix} 01 \\ 03 \\ 02 \\ 01 \end{bmatrix} \oplus x_3 \begin{bmatrix} 01 \\ 01 \\ 03 \\ 02 \end{bmatrix} \\
 &= x_0 \cdot MC_0 \oplus x_1 \cdot MC_1 \oplus x_2 \cdot MC_2 \oplus x_3 \cdot MC_3,
 \end{aligned}$$

where $MC_{i \in \{0,1,2,3\}}$ denotes the i -th column vector of MC . We call each of the right-hand side terms y_0 , y_1 , y_2 , and y_3 . The lookup table of decomposed MixColumns is then defined by Ty_i as follows:

$$\begin{aligned}
 Ty_0(x_0) &= x_0 \cdot [02 \ 01 \ 01 \ 03]^T \\
 Ty_1(x_1) &= x_1 \cdot [03 \ 02 \ 01 \ 01]^T \\
 Ty_2(x_2) &= x_2 \cdot [01 \ 03 \ 02 \ 01]^T \\
 Ty_3(x_3) &= x_3 \cdot [01 \ 01 \ 03 \ 02]^T.
 \end{aligned} \tag{1}$$

The first WB-AES implementation proposed by Chow *et al.* [10] applies 32×32 linear and two 4-bit concatenated non-linear transformations (we denote a 4-bit non-linear transformation by a nibble encoding) on the right-hand side to obfuscate key-dependent intermediate values. This encoded lookup table is commonly named *TypeII*. When the XOR lookup table to combine the output of the decomposed MixColumns is generated, no inverse linear transformation is involved because of the distributive property of matrix multiplication over logical bitwise XOR. On the other hand, the nibble encoding prevents the size of the XOR lookup table from becoming large by allowing two 4-bit inputs. This XOR lookup table is aptly named *TypeIV-II*. Next, the *TypeIII* lookup table replaces the 32×32 linear transformations applied to the *TypeII* output with 8×8 linear transformations, and the *TypeIV-III* table recombines the *TypeIII* output for the round output. By doing so, an input to the next round *TypeII* can be 8 bits thereby keeping the entire table size from becoming large. Finally, *TypeV* is a lookup table generated with the input decoding for T^{10} in the final round. Note that *TypeI* is used for the external encoding and is not considered in this paper for the interoperability of encryption and decryption operations.

Fig. 2 briefly describes *TypeIII*, *TypeIV*, and *TypeV*.

Because the vulnerabilities on the encodings that reveal the key [7, 26] two things are added in the masked WB-AES implementation. First, each byte at the right-hand side of Equation (1) is concealed by masks randomly picked for each value of $x_{i \in \{0,1,2,3\}}$. It is a customized masking method that differs from the existing masking technique that uses the same mask value. Therefore, the newly defined *TypeII-M* consists of the masked $Ty_{i \in \{0,1,2,3\}}$ values and the mask values used as shown in Fig. 1. Next, *TypeIV-IIA* combines the masked Ty_i output, and *TypeIV-IIB* produces the round output by XORing the output value of *TypeIV-IIA* and the mask used. Fig. 3 describes the table lookup overview, and this is the outline of CASE 1 [21] that provides the basic requirements of a masked WB-AES implementation.

Second, the nibble encodings are replaced by byte encodings for some inner round outputs depending on the security requirement (CASE 2 or 3). This is because the mask completely disappears in the round output after the masked MixColumns outputs are combined. However, the next section will review the DCA-variant attacks on the byte encoding and we do not use it. In this study, we propose a method to improve a masked WB-AES implementation by applying

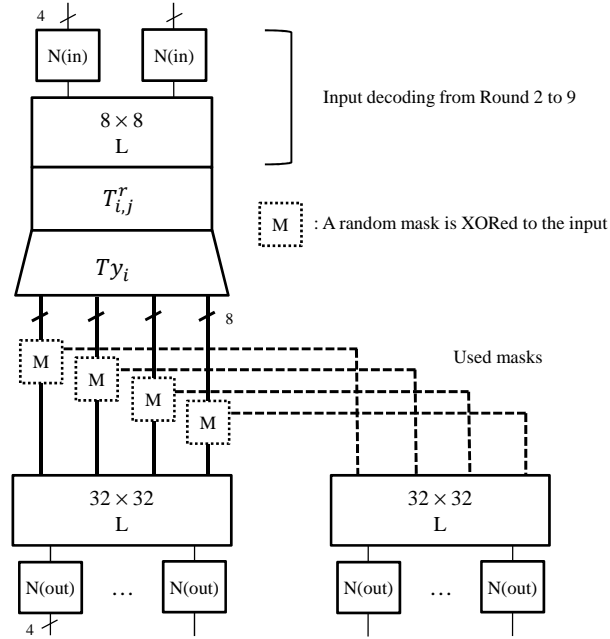


Fig. 1: *Type II-M* in the masked WB-AES implementation. L : linear transformation, N : nibble encoding/decoding.

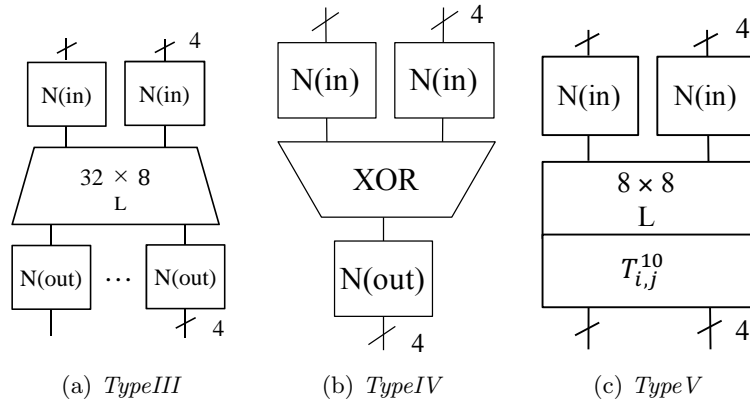
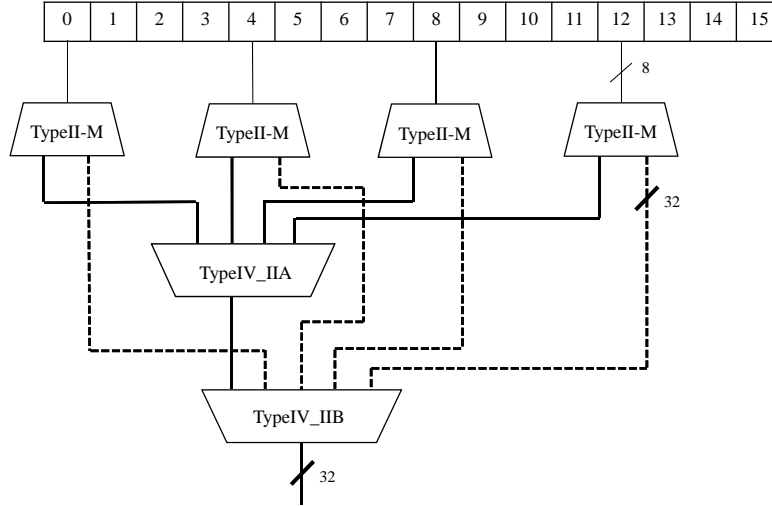
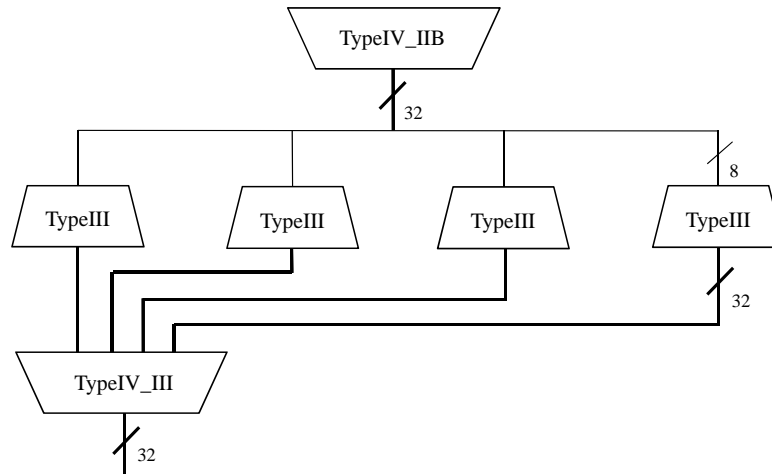


Fig. 2: Other lookup tables in CASE 1.



(a) *TypeII-M* and *TypeIV-II* tables. Dashed line: used masks. (ShiftRows omitted)



(b) *TypeIII* and *TypeIV-III* tables.

Fig. 3: Overview of table lookups in CASE 1.

masking to round output values for removing the problematic correlation without the use of byte encodings.

2.2 Walsh Transform

Consider a DCA attacker, where an attacker can know the accurate target values by accessing memory while the encryption is performed. The attacker learns the intermediate values from the computation traces, and runs a CPA attack as a subroutine to calculate the Pearson correlation with the hypothetical values. Here, a computation trace serves to provide noise-free information of intermediate values. If one can directly observe the noise-free values of intermediate values, the Walsh transform consisting of easy operations can be an alternative to CPA for evaluating the correlation [17, 26]. In this paper, we use the Walsh transform to calculate the correlation because we have generated the lookup table and all intermediate values are obtainable. The following is the definitions of the Walsh transform from [26].

Definition 1. Let $x = \langle x_1, \dots, x_n \rangle$, $\omega = \langle \omega_1, \dots, \omega_n \rangle$ be elements of $\{0, 1\}^n$ and $x \cdot \omega = x_1\omega_1 \oplus \dots \oplus x_n\omega_n$. Let $f(x)$ be a Boolean function of n variables. Then the Walsh transform of the function $f(x)$ is a real valued function over $\{0, 1\}^n$ that can be defined as $W_f(\omega) = \sum_{x \in \{0, 1\}^n} (-1)^{f(x) \oplus x \cdot \omega}$.

Definition 2. If the Walsh transform W_f of a Boolean function $f(x_1, \dots, x_n)$ satisfies $W_f(\omega) = 0$, for $0 \leq HW(\omega) \leq d$, it is called a balanced d -th order correlation immune function or an d -resilient function.

In Definition 1, let x be a hypothetical intermediate value to be analyzed and ω be the operand of the inner product with the Hamming weight (HW) 1 used to select a specific bit of x . The reason why the HW of ω is 1 is because it is difficult to analyze the key through HW or multi-bit based correlation analysis due to the encodings, whereas the single-bit analysis is successful. On the other hand, $f(x)$ represents the real lookup values and provides the noise-free intermediate values like the computation trace. To indicate a particular bit of the n -bit lookup value, $f(x)$ is represented as n Boolean functions. In Definition 2, $W_{fi} = 0$ means no correlation, whereas a large absolute value of W_{fi} means that there is a large correlation at the i -th bit of $f(x)$ and $x \cdot \omega$.

3 Vulnerability to DCA variants

This section reviews DCA and its variants on WB-AES implementations. If a white-box cryptographic algorithm is implemented without masking, DCA can break it using computation traces. If masking is applied, the key can be revealed

by extending DCA with a 2-byte key guess, or by running collision and bucketing attacks.

Before going on, we note that Higher-order DCA [6] does not work on the customized masking implementation that applies a different random mask for each value of the target intermediate value. In the case of Linear Decoding Analysis (LDA) [15], the key is analyzed by solving the system of linear equations that the matrix-unknown coefficient multiplication becomes the hypothetical intermediate value, where the matrix consists of intermediate values obtained from the corresponding computation traces. If the system is solvable for a hypothetical key, it is probably the correct key. If the system is unsolvable for every hypothetical key, then the attack fails. However, LDA is not allowed in the masked WB-AES implementation because the matrix is randomized due to the mask which makes the system unsolvable.

3.1 Power Analysis and DCA

Power analysis is a gray-box attack that recovers the key from the hypothetical intermediate value based on the fact that the power consumption is proportional or inversely proportional to the HW of the data currently being processed. A power analysis attacker calculates the hypothetical intermediate values, and statistically analyzes the value at a specific point in the power traces. The most commonly used analysis method is CPA using Pearson’s correlation coefficient. Let denote N power traces by $V_{1..N}[1..\kappa]$, and a hypothetical key by k^* , where κ is the number of sample points. For K different hypothetical keys, \mathcal{E}_{n,k^*} ($1 \leq n \leq N$, $0 \leq k^* < K$) implies the power estimate in the n -th trace. Then, the estimator r at the j -th sample point is defined as

$$r_{k^*,j} = \frac{\sum_{n=1}^N (\mathcal{E}_{n,k^*} - \overline{\mathcal{E}_{k^*}}) \cdot (V_n[j] - \overline{V[j]})}{\sqrt{\sum_{n=1}^N (\mathcal{E}_{n,k^*} - \overline{\mathcal{E}_{k^*}})^2 \cdot \sum_{n=1}^N (V_n[j] - \overline{V[j]})^2}},$$

where $\overline{\mathcal{E}_{k^*}}$ and $\overline{V[j]}$ are means of \mathcal{E}_{k^*} and $V[j]$, respectively [20]. The hypothetical key that produces the highest peak in the correlation plot is judged to be the key.

Here we note that CPA works on a white-box implementation because the linear transformation and the nibble encoding do not eliminate correlation [2, 18]. In the repository of public white-box cryptographic implementations and DCA attacks [13], DCA also uses CPA using Daredevil [8], a software tool to perform CPA. The difference from the classical power analysis is that it improves efficiency of CPA by collecting noise-free computation traces through memory access, not by collecting power traces using an oscilloscope. In average, DCA recovers 14.3 out of 16 subkeys from the Chow’s WB-AES implementation using only 200 computation traces, whereas no key is recovered from the masked WB-AES implementation [17].

As noted, masking is removed on the round output in the masked implementation. Therefore, the round output values can be attacked in various ways. From

now on, we introduce those attacks on non-masked round outputs. We begin with DCA with a 2-byte key guess [25]. Each subbyte of the first round output of AES-128 is associated with four subkeys, so the size of the key space is 2^{32} when a brute-force is carried out for guessing a byte. To reduce this complexity to 2^{16} , two bytes in a column of the plaintext state can be fixed to zero or a some value. For example, if (x_0, x_1, x_2, x_3) is the first column of the plaintext state and if x_0, x_1 are fixed to 0, the first byte of the round output can be written as $s = S(x_2 \oplus k_{2,2}^0) \oplus S(x_3 \oplus k_{3,3}^0) \oplus c$ for some constant c . Then, DCA with 2^{16} key space is successful because $S(x_2 \oplus k_{2,2}^0) \oplus S(x_3 \oplus k_{3,3}^0)$ is correlated to s which is in turn correlated to its encoded value.

3.2 Collision Attack

By fixing two input bytes, a collision attack [25] can also be mounted with 2^{16} key space. This is similar to the principle of 2-byte key guess described earlier, and is based on the fact that if a hypothetical subbyte of the round output collides for a pair of inputs, so does its encoded value in the computation trace. For each pair of inputs and their computation traces, an attacker compares the values of each sample position in the two traces and gives 1 if the two values are equal, and 0 if they are different, to generate a collision computation trace (CCT). Similarly, the collision prediction is composed of 0 and 1 which are assigned in the same way by comparing two hypothetical subbytes of the round outputs for each pair of the inputs and a key guess. Thus, there is a perfect match between the target sample position in the CCT and the collision prediction for the correct hypothetical key. Here we do not take into account the improved mutual information analysis [25] because this is similar to the collision in many respects and succeeds if and only if the collision attack succeeds.

3.3 Bucketing Attack

Extended statistical bucketing analysis [28], as a variant of the collision attack, is based on the fact that if two correct hypothetical intermediate values for a pair of plaintexts do not collide, their corresponding encoded values should not collide as well. For example, an attacker can divide the first subbyte of plaintexts into two sets with two distinct values for the lower four bits of the S-box output. By fixing the remaining 15 subbytes of the plaintext, the attacker can be convinced that the two sets of plaintexts produce disjoint sets of the lower four bits of the first subbyte in the first round output. This attack works on a WB-AES implementation due to the use of the nibble encoding. Thus, this attacker can confirm or deny a hypothetical key by observing whether or not the first subbyte in the round output is disjoint depending on the chosen-plaintext set. Bucketing Computational Analysis (BCA) uses computation traces to apply this principle to white-box cryptography.

Zero Difference Enumeration (ZDE) [3] may also be considered similar to BCA. ZDE works by selecting special pairs of plaintexts that allow the significant number of intermediate values computed by the correct hypothetical key to be

identical. However, this is known to be inefficient taking 500×2^{18} traces to recover a subkey of AES, and also the selected pairs of plaintexts are unable to make identical intermediate values in the masked WB-AES implementation.

4 Proposed Method

Most of DCA-variant attacks on the previous masked WB-AES implementation analyze the round output in which the masks are removed. In this section, we propose a method to provide the masked round output and unmask it in the input decoding phase of the next round. The following explains how to modify *TypeII* and *TypeV*, depending on the presence or absence of masked inputs and outputs, and how to connect to other tables.

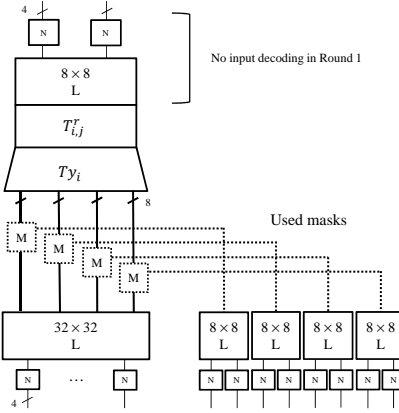
TypeII_MO (Masked Out). This puts the random masks on the Ty_i output value, encodes the masked value and the mask used. This is used in the first round because each subbyte of the first round output only involves 32 bits of the key. Note that all 128 bits of the key affect each subbyte of the round output after the output value of the second MixColumns multiplication is XORed. For the same reason, this is also used in the eighth round because each subbyte of the ninth round input needs to be protected by masking, as only six bytes of the key are associated with it in terms of decryption that goes back from ciphertexts.

The difference from *TypeII-M* used in the previous masked WB-AES implementation is the method of encoding masks. As shown in Fig. 1 and Fig. 3, the masked Ty_i values were previously unmasked before the *TypeIII* lookup, and thus the intermediate value and the mask share the same matrix for the linear transformation in order to take advantage of the distributive property of matrix multiplication over XOR.

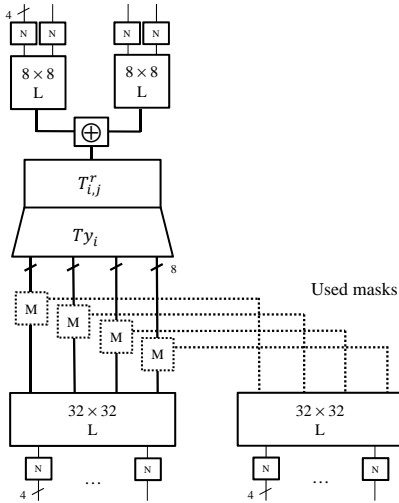
In this work, the mask is not immediately combined with the masked Ty_i lookup values, but with the other mask values to provide the masked round output. Fig. 4a shows that 8×8 linear transformations are used on the mask in *TypeII_MO* because the masks are joined together between masks. This is because the mask itself is a random value generated in a uniform distribution and independent of the key, so there is no reason to apply a linear transformation of large diffusion effects. For this reason, the masks do not require the process of replacing linear transformations by *TypeIII* and *TypeIV_III*, thus reducing the overall table size and the number of lookups.

Let denote *TypeIV_IIM* the *TypeIV* table used to combine the mask outputs from *TypeII_MO* which is represented by dotted lines. Then, the *TypeIV_II* table combines only the masked Ty_i values and prepares a masked round output as shown in Fig. 5a.

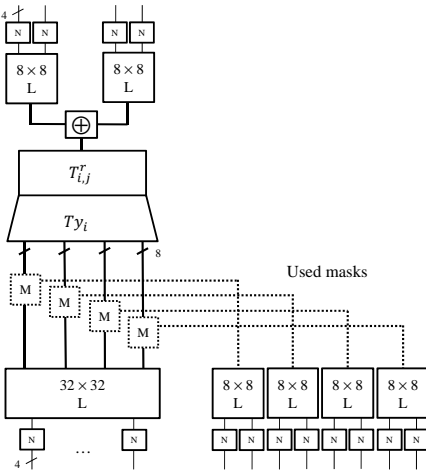
After computing the masked round output above, we replace the 32×32 linear transformation applied to it with 8×8 linear transformations using *TypeIII* and *TypeIV_III* like in the case of Chow’s WB-AES implementation. Then we have two 4×4 state matrices, *vs* (value state) and *ms* (mask state), where *vs* is the masked round output and *ms* is the mask value. This lookup sequence is illus-



(a) *TypeII_MO*. No input decoding is performed for the first round because there is no external encoding.



(b) *TypeIIMIMO* in the second round.



(c) *TypeIIMIMO* in the ninth round.

Fig. 4: Modified *TypeII* tables for the masked outputs.

trated in Fig. 8a.

TypeII_MIMO (Masked In Masked Out). Because the first round output is masked, the *TypeII* table of the second round takes each byte of *vs* and *ms* as input, decodes and XORs each other. The result is a subbyte of the first round output and an input to T^2 at the same time. As explained, all bits of the key are not associated with each intermediate byte until the output value of the second round MixColumns is combined. Therefore, masking is again applied to the second round Ty_i values to protect them.

Here, we call it *TypeII_MIMO*, which takes the masked input and provides the masked Ty_i values. *TypeII_MIMO* is again divided into two types, depending on the linear transformation applied to the mask. If the masked round output is unmasked before looking up the *TypeIII* table, like in the case of the previous masked WB-AES implementation shown in Fig. 3a, a 32×32 linear transformation is applied. Otherwise, if the masked round output and the mask values are separated into *vs* and *ms*, and passed to the next round, an 8×8 linear transformation is applied. In the second round, the XOR operations between the masked Ty_i values keep the intermediate values masked until each subbyte of the round output is computed. For this reason, a 32×32 linear transformation is applied to the mask in the second round as represented in Fig. 4b for the unmasking through *TypeIV* lookups as shown in Fig. 5b. The overall sequence of table lookups in the second round is shown in Fig. 8b.

On the other hand, each subbyte of the ninth round output needs to be masked. This is because if the two subkeys hidden in T^{10} of the final round are correctly guessed by the attacker, the hypothetical subbyte of the ninth round output computed inversely from the ciphertext will correlate with the corresponding subbyte of the encoded ninth round output. Thus, the masked Ty_i values and the masks are XORed separately and passed to the input of *TypeV_MI* in the final round as shown in Fig. 5c and Fig. 8c. By abuse of notation, we continue to use the same names for *TypeII_MIMO* and *TypeIV_IIM* in the second and ninth rounds for the simplicity although they differ in the linear transformation applied to the mask and the number of copies of the *TypeIV* table, respectively. The size of each table and the number of lookups are analyzed in the next section.

TypeII. The *TypeII* table (Fig. 6) for the rest of the inner rounds (third to seventh) is used like in the case of Chow's WB-AES implementation, as masking is not applied to inputs and outputs. The replacement of linear transformations are normally processed by *TypeIII* and *TypeIV_III* as depicted in Fig. 8d.

TypeV_MI (Masked In). For the final round, the *TypeV_MI* table is generated in such a way to take each byte from *vs* and *ms*, decode, and then XOR them. This result value will be an input byte to T^{10} as shown in Fig. 7. Without the external encoding, each *TypeV_MI* output becomes a subbyte of the ciphertext (Fig. 8e).

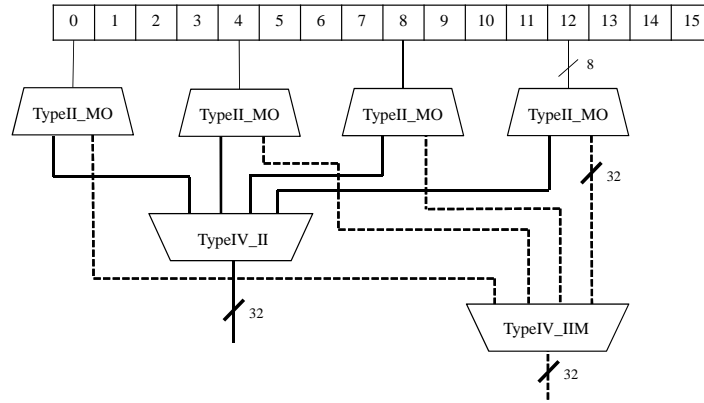
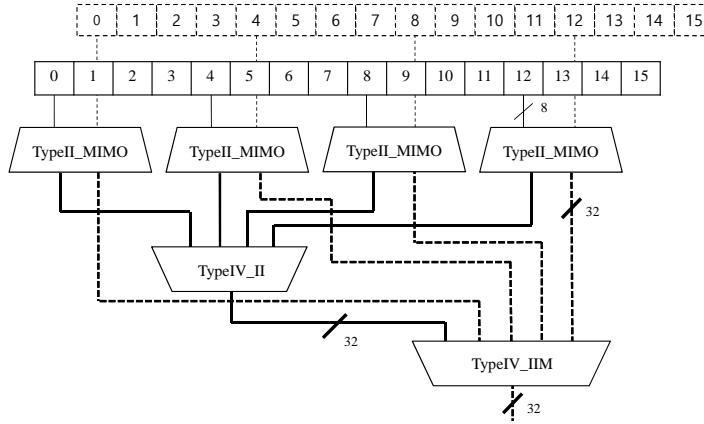
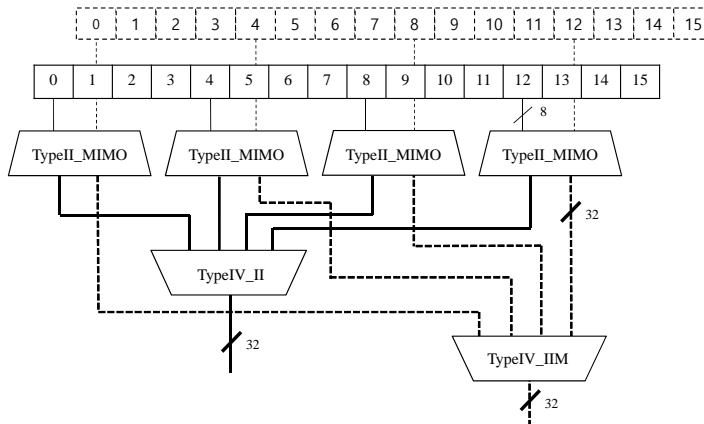
(a) *TypeII_MO* and *TypeIV* in the first and eighth rounds.(b) *TypeII_MIMO* and *TypeIV* in the second round.(c) *TypeII_MIMO* and *TypeIV* in the ninth round.

Fig. 5: Masked round output and XOR. Solid line: masked value. Dotted line: mask.

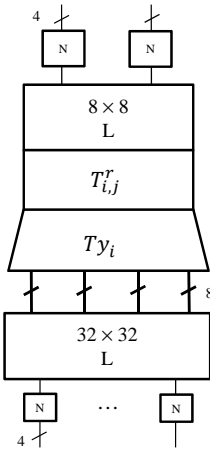


Fig. 6: *Type II* used in the inner rounds [10].

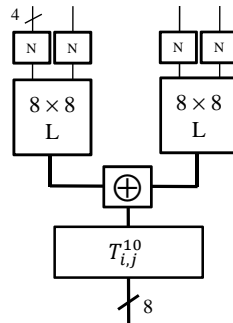


Fig. 7: *Type V.MI* in the final round.

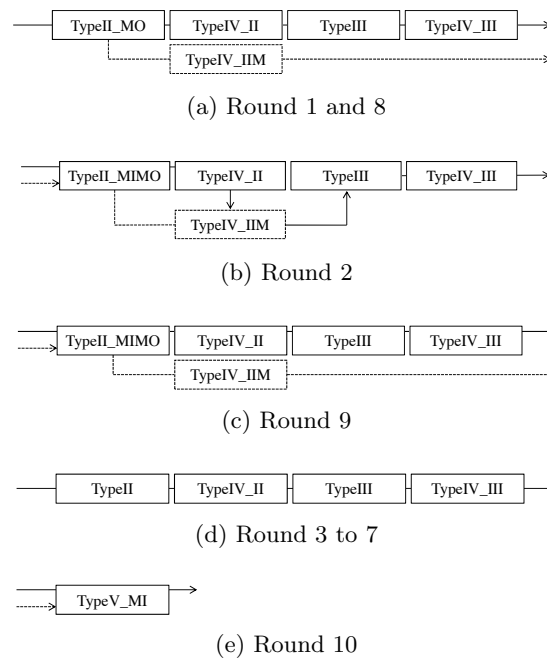


Fig. 8: Lookup sequence for each round. Solid arrow: masked value. Dotted arrow: mask.

5 Evaluation

We evaluate our proposed method in terms of security and performance. To be specific, we demonstrate protection against of DCA and DCA variants described in Section 3, and analyze the table size and the number of lookups. Briefly speaking, we have generated the lookup tables following the proposed WB-AES implementation, and conducted various experiments. First, the correlation between the *TypeII_MO* lookup value and the hypothetical value of the SubBytes output in the first round is analyzed with the Walsh transform. In addition, the correlation between the masked round output and the hypothetical round output computed by the 2-byte key guess is also analyzed. Next, a perfect match for a collision attack is tested on the masked round output. Finally, we check if the chosen plaintexts of the bucketing attacker can make disjoint sets on the masked round output when the hypothetical key is correct.

5.1 Security analysis and Experimental Results

We analyze and demonstrate hereafter the protection against the vulnerabilities explained in Section 3. We first show protection against DCA on the *TypeII_MO* outputs in the first round. In fact, masking of the Ty_i output in the first round is not different from the previous implementation [17], that had been proven to defend against DCA. So we calculated the correlation by using the Walsh transform in Section 2. For the first subbyte $p \in \{0,1\}^8$ of the plaintext and a hypothetical subkey k , the correlation between each bit of the hypothetical S-box output and its corresponding *TypeII_MO* values can be quantified by

$$W_{f_i}(\omega) = \sum_{p \in \{0,1\}^8} (-1)^{f_i(p) \oplus \{s(p \oplus k) \cdot \omega\}},$$

where $f_i(p)$ is the i -th bit of the left 32-bit value of the *TypeII_MO* output shown in Fig. 4a. Because this equation tests all possible values of p and $f_i(p)$ is obtainable, the correlation can be analyzed accurately as if it is analyzed using a large number of random plaintexts. Fig. 9 is the result of the Walsh transform for the first subkey and shows that the key leakage did not occur when each bit of the SubBytes output and each bit of the *TypeII_MO* output were analyzed. A DCA attack using 10,000 software traces also failed as shown in TABLE 1.

Second, a DCA attack with a 2-byte key guess can be protected. As explained previously, the first subbyte of the round output without masking can be represented by a function of p_2 and p_3 as:

$$s(p_2, p_3) = S(p_2 \oplus k_{2,2}^0) \oplus S(p_3 \oplus k_{3,3}^0) \oplus c$$

if the attacker fixes the first two bytes to zero in the first column of the plaintext state. In the case of the masked round output, this can be written as:

$$\hat{s}(p_2, p_3) = s(p_2, p_3) \oplus r_2(p_2) \oplus r_3(p_3) \oplus c_r,$$

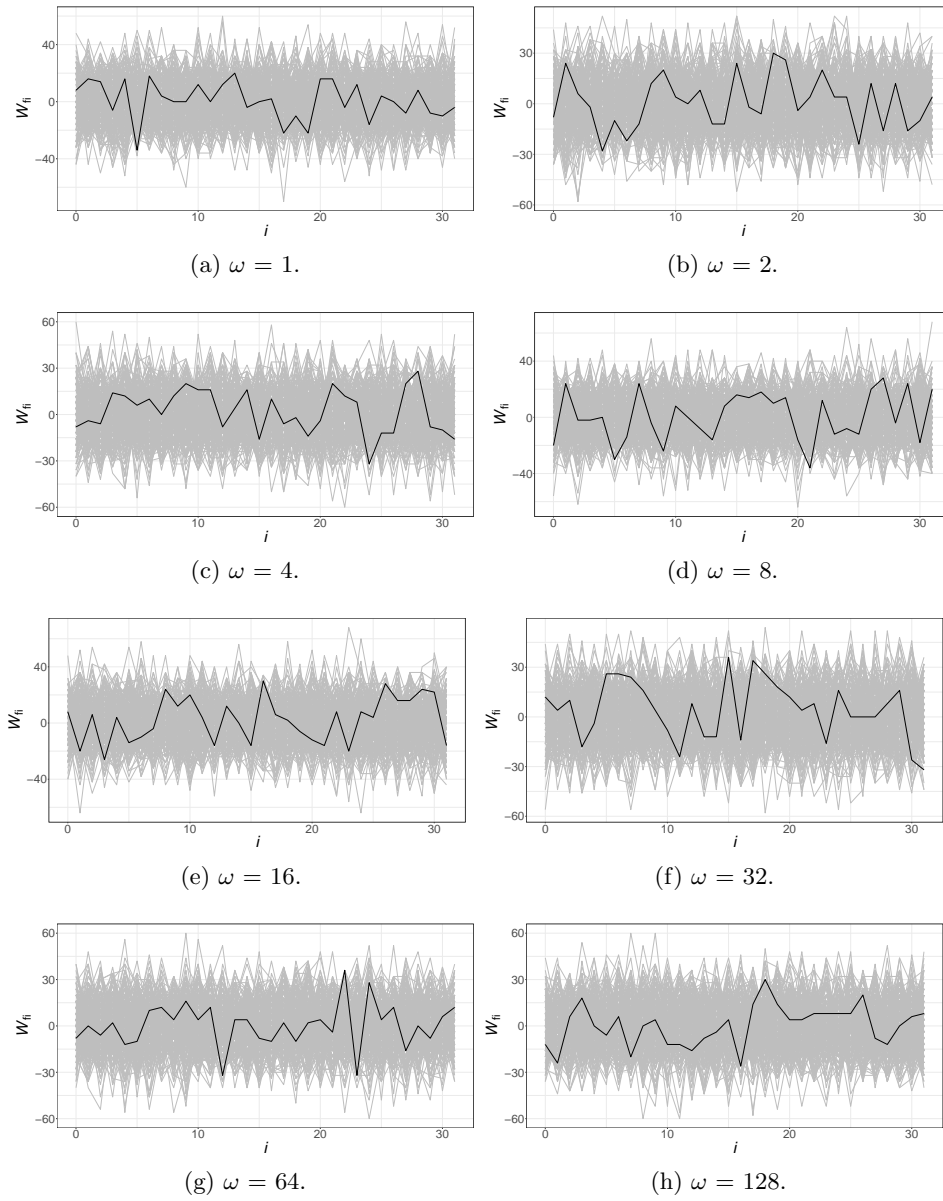


Fig. 9: The Walsh transforms on the *TypeII-MO* outputs (except the mask) in the first round. Black: correct key; gray: wrong key.

Table 1: DCA ranking for the proposed WB-AES implementation when conducting mono-bit CPA on the SubBytes output in the first round with 10,000 software traces.

TargetBit	SubKey															
	1	2	3	4	5	6	7	8	9	10	11	12	13	14	15	16
1	216	5	39	111	148	132	176	199	246	66	69	104	25	86	72	208
2	191	174	116	72	219	18	67	3	15	226	178	240	146	196	151	121
3	90	144	170	201	182	4	29	81	166	120	237	124	227	159	216	226
4	251	91	185	150	218	2	142	39	97	50	132	8	81	157	229	185
5	45	173	192	101	10	146	45	33	177	206	136	14	135	71	22	234
6	191	146	101	121	146	93	188	60	234	28	165	38	201	244	236	88
7	38	252	16	188	105	222	185	69	124	21	50	100	44	101	3	215
8	39	98	97	252	124	138	88	46	219	130	193	230	20	30	29	194

where c_r is a fixed mask for c , and r_2 and r_3 are random bijections which act like random mask selection with uniform distributions. By representing $r_2(p_2) \oplus r_3(p_3) \oplus c_r \oplus c$ as $r(p_2, p_3)$, a function of p_2 and p_3 , we have

$$\hat{s}(p_2, p_3) = S(p_2 \oplus k_{2,2}^0) \oplus S(p_3 \oplus k_{3,3}^0) \oplus r(p_2, p_3).$$

This can be rewritten as shown below by substituting the correct subkeys for $k_{2,2}^0$ and $k_{3,3}^0$:

$$\hat{s}(p_2, p_3) = S(p_2 \oplus 0xAA) \oplus S(p_3 \oplus 0xFF) \oplus r(p_2, p_3).$$

Then the first subbyte of the first round output obtained from *TypeIV_II* can be expressed by $\epsilon(\hat{s}(p_2, p_3)) = \epsilon \circ \hat{s}(p_2, p_3)$, where ϵ is an encoding of the round output. Let's assume that the attacker already knows the subkey $k_{2,2}^0 = 0xAA$, and the hypothetical value is given by $h(p_2, p_3, k)$ as follows:

$$h(p_2, p_3, k) = S(p_2 \oplus 0xAA) \oplus S(p_3 \oplus k),$$

where k is a hypothetical subkey. Then the correlation between $\epsilon(\cdot)$ and $h(\cdot)$ can be quantified by

$$W_{\epsilon_i}(\omega) = \sum_{p_2 \in \{0,1\}^8} \sum_{p_3 \in \{0,1\}^8} (-1)^{\epsilon_i(\hat{s}(p_2, p_3)) \oplus \{h(p_2, p_3, k) \cdot \omega\}},$$

where $\epsilon_i(\cdot)$ is the i -th bit of $\epsilon(\cdot)$. Here we can know that $\hat{s}(\cdot)$ will no longer correlate to $h(\cdot)$ if $r(p_2, p_3)$ generates a random byte with a uniform distribution. Our experimental result shows that DCA with a 2-byte guess cannot succeed even if the attacker is able to correctly guess the remaining subkey $k = 0xFF$ as shown in Fig. 10. In other words, this means that $\hat{s}(\cdot)$ is not correlated to $h(\cdot, k^*)$ due to the random masks, where k^* denotes the correct subkey.

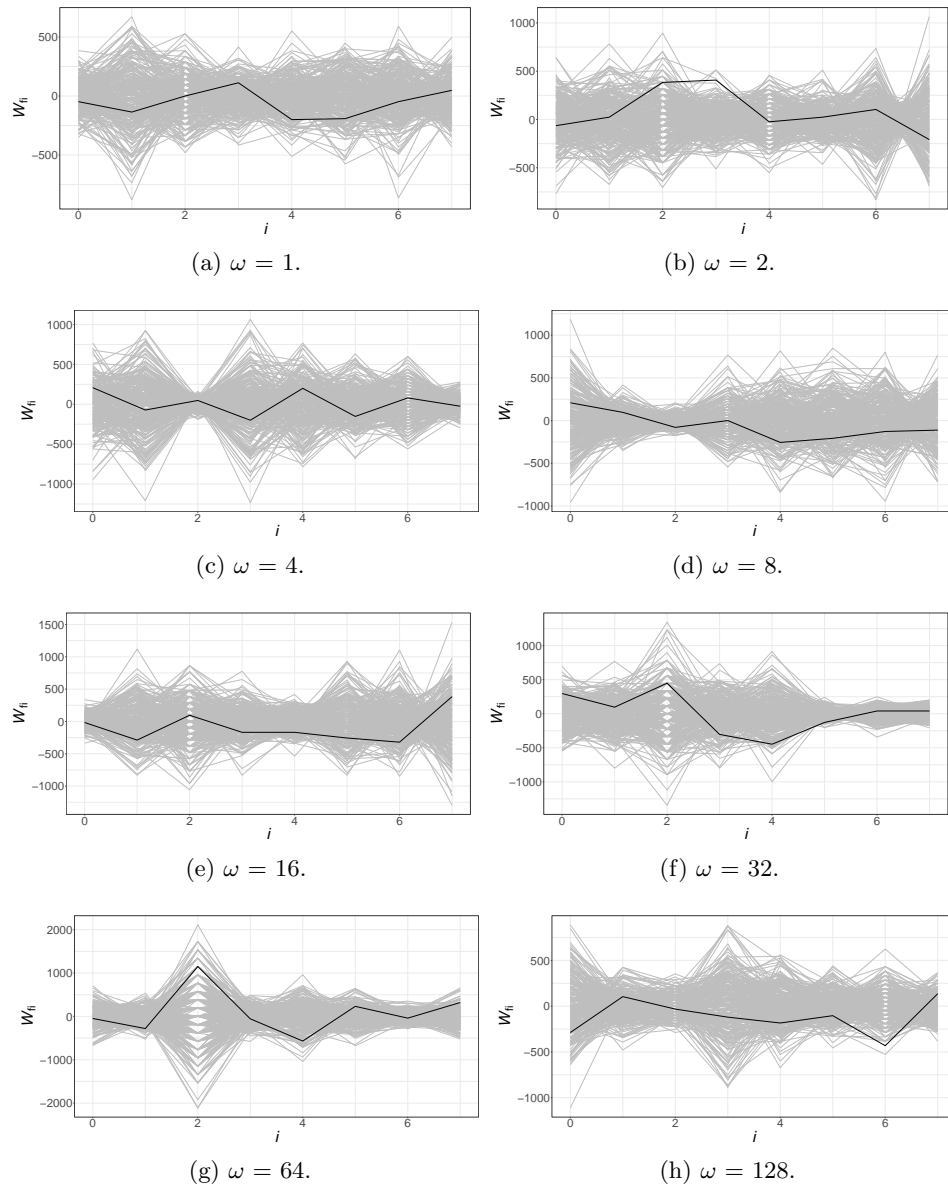


Fig. 10: The Walsh transforms on the masked round output in the first round. Black: correct key; gray: wrong key.

Third, the collision attack is also not allowed because the perfect match between the hypothetical value computed from the correct hypothetical key and the target sample in the CCT will be violated in the masked round output. For four positive

integers $a, b, c, d \in \{0, 1\}^8$, suppose that $h(a, b, k^*) = h(c, d, k^*)$. Then, the perfect match for the collision attack is valid if and only if $\epsilon(\hat{s}(a, b)) = \epsilon(\hat{s}(c, d))$ which in turn means $\hat{s}(a, b) = \hat{s}(c, d)$ because ϵ is deterministic and bijective. However, we know that $\Pr[\hat{s}(a, b) = \hat{s}(c, d)] = 1/256$ because $\Pr[r(a, b) = r(c, d)] = 1/256$, and thus the perfect match is not guaranteed.

We have collected the following set of pairs:

$$\mathcal{I}_v = \{(a, b) : a, b \in \{0, 1\}^8 | h(a, b, k^*) = v, \text{ for } v \in \{0, 1\}^8\}.$$

Consider a vector $Z_v = [z^1 z^2 \dots z^\ell]$ defined as:

$$z^i = \epsilon(s(a^i, b^i)), \forall (a^i, b^i) \in \mathcal{I}_v,$$

where $\ell = |\mathcal{I}_v|$. Let Z_* denote a vector consisting of ℓ identical constants. The perfect match for the successful collision attack requires $z^1 = z^2 = \dots = z^\ell$ in Z_v , and the cosine similarity between Z_* and Z_v should be 1 because $\cos(0^\circ) = 1$. Indeed, Fig. 11a shows that the correct subkey shows the cosine similarity 1 when the round output is not masked. This implies the success of the collision attack. To evaluate the effect of adding the mask on the round output, we have generated the vector Z'_v as follows:

$$z^i = \epsilon(\hat{s}(a^i, b^i)), \forall (a^i, b^i) \in \mathcal{I}_v.$$

Then, the cosine similarity between Z_* and Z'_v for the correct subkey looks random like other wrong hypothetical subkeys as shown in Fig. 11b. This implies that the masked round output protects against the collision attack.

Finally, the bucketing attack can be also protected. Before going on, we begin with a demonstration of how it works on the previous WB-AES implementation. For two bucket nibbles $d_0, d_1 \in \{0, 1\}^4$ such that $d_0 \neq d_1$, a bucketing attacker defines two sets:

$$\mathcal{J}_{d_i} = \{p \in \{0, 1\}^8 | s(p \oplus k) \& 0xF = d_i\},$$

where $i \in \{0, 1\}$, and k is a hypothetical key. Let $[0 \ 0 \ p \ 0]^T$ be the first column of the plaintext state, where $p \in \{0, 1\}^8$. Then the lower 4 bits of the first subbyte in the first round output of AES-128 can be written as:

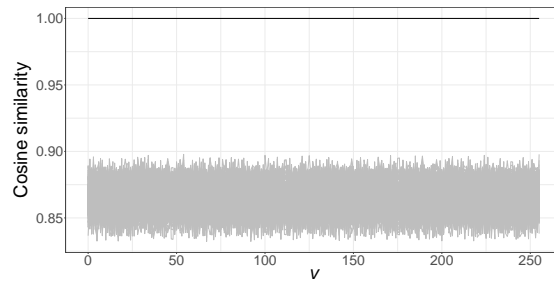
$$g(p) = (s(p \oplus k^*) \oplus c) \& 0xF.$$

The bucketing attack is based on the fact that a correct key guarantees that $\mathcal{B}_{b_0} \cap \mathcal{B}_{b_1} = \emptyset$, where

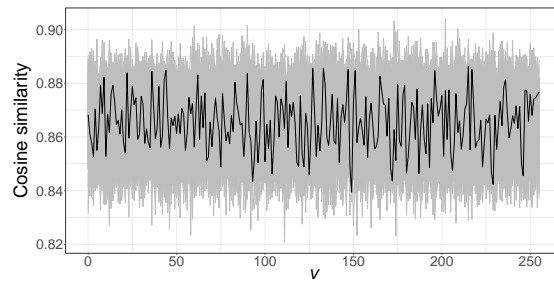
$$\mathcal{B}_{b_i} = \{b_i | \forall p \in \mathcal{J}_{d_i}, g(p) = b_i\}.$$

Consider only the nibble encoding denoted by δ on the round output without applying linear transformations:

$$g^\delta(p) = \delta(s(p \oplus k^*) \oplus c) \& 0xF.$$



(a) Between Z_* and Z_v without round output masking.



(b) Between Z_* and Z'_v with round output masking.

Fig. 11: Cosine similarity without and with masking on the round output. Black: correct key, gray: wrong key.

Then, one can easily know that $\mathcal{B}_{b_0}^\delta \cap \mathcal{B}_{b_1}^\delta = \emptyset$, where

$$\mathcal{B}_{b_i}^\delta = \{b_i | \forall p \in \mathcal{J}_{d_i}, g^\delta(p) = b_i\},$$

For $index = d_0 || d_1$, such that $d_0 < d_1$ (for removing duplicated bucket nibbles), our experimental result depicted in Fig. 12a shows that the correct key always guarantees that $\mathcal{B}_{b_0}^\delta$ and $\mathcal{B}_{b_1}^\delta$ are disjoint. This is in contrast to a result of $\mathcal{B}_{b_0}^\epsilon$ and $\mathcal{B}_{b_1}^\epsilon$ shown in Fig. 12b which have a number of intersection elements due to linear transformation providing the diffusion effect, where

$$g^\epsilon(p) = \epsilon(s(p \oplus k^*) \oplus c) \& 0xF$$

and

$$\mathcal{B}_{b_i}^\epsilon = \{b_i | \forall p \in \mathcal{J}_{d_i}, g^\epsilon(p) = b_i\}.$$

Here, the bucketing attacker can find a key that most frequently makes $\mathcal{B}_{b_0}^\epsilon \cap \mathcal{B}_{b_1}^\epsilon = \emptyset$, because the wrong hypothetical keys have never produced an empty set. Fig. 12c shows that the correct key (*0xAA*) has 96 indexes (out of 120) that lead to a disjoint set, and the other wrong hypothetical keys never make one.

To evaluate the effect of the masked round output against the bucketing attack, we define \hat{g} for the lower 4 bits of the first subbyte in the masked round output as follows:

$$\hat{g}(p) = \epsilon(s(p \oplus k^*) \oplus c \oplus r(p) \oplus c_r) \& 0xF.$$

For each plaintext set \mathcal{J}_{d_i} , we have collected the target 4 bits into the set $\hat{\mathcal{B}}_{b_i}$ defined as:

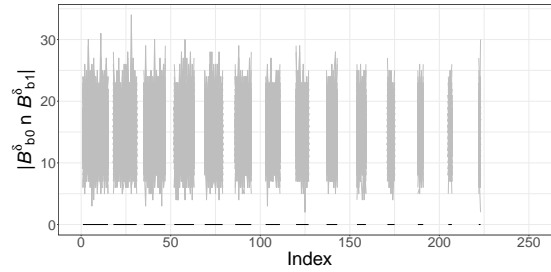
$$\hat{\mathcal{B}}_{b_i} = \{b_i | \forall p \in \mathcal{J}_{d_i}, \hat{g}(p) = b_i\}.$$

Because $r(p)$ generates random numbers, our experiment result shows that $\hat{\mathcal{B}}_{b_0}$ and $\hat{\mathcal{B}}_{b_1}$ are never disjoint for any pair of (d_0, d_1) , where $d_0 < d_1$. Thus, the bucketing attack does not work on the proposed method.

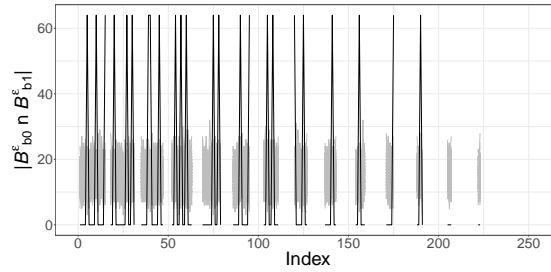
5.2 Performance

The total table size of our implementation is calculated as follows:

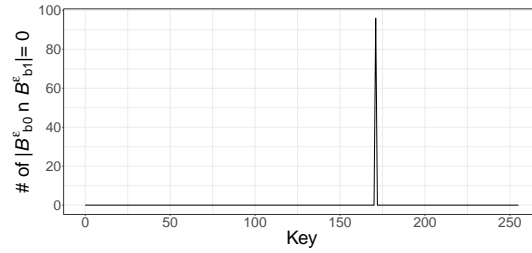
- *TypeII_MO* : $2 \times 4 \times 4 \times 256 \times 4 \times 2 = 65,536$
- *TypeII_MIMO* : $2 \times 4 \times 4 \times 256 \times 256 \times 4 \times 2 = 16,777,216$
- *TypeII* : $5 \times 4 \times 4 \times 256 \times 4 = 81,920$
- *TypeIV_IIM* : $3 \times 4 \times 4 \times 3 \times 2 \times 128 = 36,864$
- *TypeIV_IIM* : $4 \times 4 \times 4 \times 2 \times 128 = 16,384$
- *TypeIV_II* : $9 \times 4 \times 4 \times 3 \times 2 \times 128 = 110,592$
- *TypeIII* : 147,456
- *TypeIV_III* : 110,592
- *TypeV_MI* : $4 \times 4 \times 256 \times 256 = 1,048,576$



(a) With only the nibble encoding.

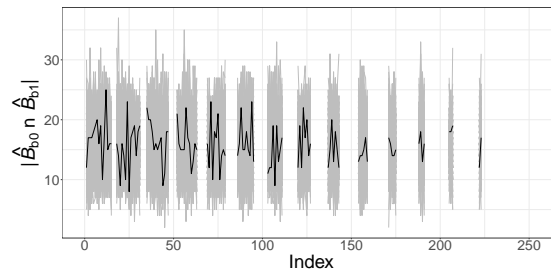


(b) With the nibble encoding and the linear transformation.

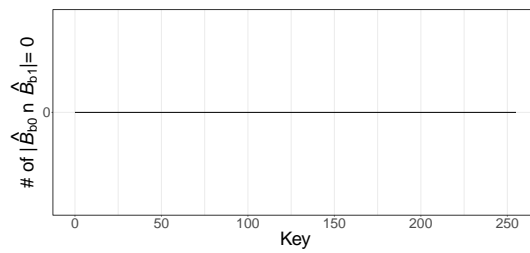


(c) Number of indexes making a disjoint set for each key.

Fig. 12: Bucketing attack on the previous WB-AES implementation. Black: correct key, gray: wrong key. $Index = d_0 \parallel d_1$ such that $d_0 < d_1$. The other indexes are undefined.



(a) No disjoint sets for any pair of (d_0, d_1) , where $d_0 < d_1$. Black: correct key, gray: wrong key.



(b) Number of indexes making a disjoint set for each key. All are 0.

Fig. 13: Bucketing attack on the masked round output.

Thus the total size is 18,395,136 bytes (approximately 17.5 MB). The reason the table size has increased compared to the previous one is the use of tables that take a two-byte input. This total size is roughly 35.3 times and 3.7 times larger than Chow’s WB-AES and the CASE 3 implementation of the previous masked WB-AES, respectively, but there is a difference in the range of target attacks and protected rounds.

Note that we do not compare with CASE 1 and CASE 2 in the previous version of the masked implementation because these provide only partial protection.

The number of table lookups are counted as follows.

- *TypeI_LMO* : $2 \times 4 \times 4 \times 2 = 64$
- *TypeI_LMIMO* : $2 \times 4 \times 4 \times 2 = 64$
- *TypeII* : $5 \times 4 \times 4 = 80$
- *TypeIV_IIM* : $3 \times 4 \times 4 \times 3 \times 2 = 288$
- *TypeIV_IIM* : $4 \times 4 \times 4 \times 2 = 128$
- *TypeIV_II* : $9 \times 4 \times 4 \times 3 \times 2 = 864$
- *TypeIII* : $9 \times 4 \times 4 = 144$
- *TypeIV_III* : $9 \times 4 \times 4 \times 3 \times 2 = 864$
- *TypeV_MI* : $4 \times 4 = 16$

Then, these are 2,512 lookups in total. This is 1.2 times and 0.7 times compared to Chow’s WB-AES and the CASE 3 implementation of the previous masked WB-AES, respectively. As a result, there is little difference in the number of lookups. Because of the relatively large size of the table, available memory space on the target device should be considered.

6 Conclusion and Discussion

Previously, a white-box cryptographic implementation was combined with the masking technique to protect against DCA attacks. This implementation eliminated all masks from the round output and used byte encoding instead of nibble encoding, which resulted in vulnerabilities to DCA-variant attacks. In this paper, we also applied masking techniques to the round output values, as a way to depend against existing DCA variants. Based on the previous masked WB-AES implementation, the several round outputs were masked and each mask was removed in the input decoding of the next round. Our security evaluation showed that this method can protect against DCA with a 2-byte key guess, collision and bucketing attacks.

The downside of this work is the memory requirement that is nearly four times larger than the previous masked WB-AES implementation. For this reason, it will not be applicable to low-cost devices that have only a few hundred KB of memory. However, it can be used in smart devices that provide enough memory space. In fact, there is no serious problem with execution speed because the number of table lookups is not large. As a future work, this method has to combine protection techniques for cryptanalysis in order to protect priceless information.

References

1. Akkar, M., Giraud, C.: An Implementation of DES and AES, Secure against Some Attacks. In: Cryptographic Hardware and Embedded Systems - CHES 2001, Third International Workshop, Paris, France, May 14-16, 2001, Proceedings. pp. 309–318. No. Generators (2001), http://dx.doi.org/10.1007/3-540-44709-1_26
2. Alpirez Bock, E., Brzuska, C., Michiels, W., Treff, A.: On the Ineffectiveness of Internal Encodings - Revisiting the DCA attack on White-box Cryptography. In: Applied Cryptography and Network Security - 16th International Conference, ACNS 2018, Proceedings. pp. 103–120. Lecture Notes in Computer Science (including sub-series Lecture Notes in Artificial Intelligence and Lecture Notes in Bioinformatics), Springer, Germany (1 2018)
3. Banik, S., Bogdanov, A., Isobe, T., Jepsen, M.B.: Analysis of Software Countermeasures for Whitebox Encryption. vol. 2017, pp. 307–328 (2017), <http://tosc.iacr.org/index.php/ToSC/article/view/596>
4. Billet, O., Gilbert, H., Ech-Chatbi, C.: Cryptanalysis of a White Box AES Implementation. In: Selected Areas in Cryptography, 11th International Workshop, SAC 2004, Waterloo, Canada, August 9-10, 2004, Revised Selected Papers. pp. 227–240 (2004), http://dx.doi.org/10.1007/978-3-540-30564-4_16
5. Blömer, J., Guajardo, J., Krummel, V.: Provably Secure Masking of AES. In: Selected Areas in Cryptography, 11th International Workshop, SAC 2004, Waterloo, Canada, August 9-10, 2004, Revised Selected Papers. pp. 69–83 (2004), http://dx.doi.org/10.1007/978-3-540-30564-4_5
6. Bogdanov, A., Rivain, M., Vejre, P.S., Wang, J.: Higher-Order DCA against Standard Side-Channel Countermeasures. In: Polian, I., Stöttinger, M. (eds.) Constructive Side-Channel Analysis and Secure Design - 10th International Workshop, COSADE 2019, Darmstadt, Germany, April 3-5, 2019, Proceedings. Lecture Notes in Computer Science, vol. 11421, pp. 118–141. Springer (2019), https://doi.org/10.1007/978-3-030-16350-1_8
7. Bos, J.W., Hubain, C., Michiels, W., Teuwen, P.: Differential Computation Analysis: Hiding your White-Box Designs is Not Enough. vol. 2015, p. 753 (2015), <http://dblp.uni-trier.de/db/journals/iacr/iacr2015.html#BosHMT15>
8. Bottinelli, P., Bos, J.W.: Computational Aspects of Correlation Power Analysis (2015), <https://eprint.iacr.org/2015/260>
9. Brier, E., Clavier, C., Olivier, F.: Correlation Power Analysis with a Leakage Model. In: Cryptographic Hardware and Embedded Systems - CHES 2004: 6th International Workshop Cambridge, MA, USA, August 11-13, 2004. Proceedings. Lecture Notes in Computer Science, vol. 3156, pp. 16–29. Springer (2004)
10. Chow, S., Eisen, P., Johnson, H., Oorschot, P.C.V.: White-Box Cryptography and an AES Implementation. In: Proceedings of the Ninth Workshop on Selected Areas in Cryptography (SAC 2002). pp. 250–270. Springer-Verlag (2002)
11. Chow, S., Eisen, P.A., Johnson, H., van Oorschot, P.C.: A White-Box DES Implementation for DRM Applications. In: Security and Privacy in Digital Rights Management, ACM CCS-9 Workshop, DRM 2002, Washington, DC, USA, November 18, 2002, Revised Papers. pp. 1–15 (2002), http://dx.doi.org/10.1007/978-3-540-44993-5_1
12. Coron, J., Goubin, L.: On Boolean and Arithmetic Masking against Differential Power Analysis. In: Cryptographic Hardware and Embedded Systems - CHES 2000, Second International Workshop, Worcester, MA, USA, August 17-18, 2000, Proceedings. pp. 231–237 (2000), http://dx.doi.org/10.1007/3-540-44499-8_18

13. Deadpool. A repository of various public white-box cryptographic implementations and their practical attacks.: <https://github.com/SideChannelMarvels/Deadpool/>
14. Goubin, L., Masereel, J., Quisquater, M.: Cryptanalysis of White Box DES Implementations. In: Selected Areas in Cryptography, 14th International Workshop, SAC 2007, Ottawa, Canada, August 16-17, 2007, Revised Selected Papers. pp. 278–295 (2007), http://dx.doi.org/10.1007/978-3-540-77360-3_18
15. Goubin, L., Paillier, P., Rivain, M., Wang, J.: How to Reveal the Secrets of an Obscure White-Box Implementation. IACR Cryptology ePrint Archive 2018, 98 (2018), <http://eprint.iacr.org/2018/098>
16. Joye, M.: On WhiteBox Cryptography (2008), <http://joye.site88.net/papers/Joy08whitebox.pdf>
17. Lee, S., Kim, T., Kang, Y.: A Masked White-Box Cryptographic Implementation for Protecting Against Differential Computation Analysis. IEEE Transactions on Information Forensics and Security 13(10), 2602–2615 (Oct 2018)
18. Lee, S., Jho, N., Kim, M.: On the Key Leakage from Linear Transformations (2018), <https://eprint.iacr.org/2018/1047.pdf>
19. Lepoint, T., Rivain, M., Mulder, Y.D., Roelse, P., Preneel, B.: Two Attacks on a White-Box AES Implementation. In: Selected Areas in Cryptography - SAC 2013 - 20th International Conference, Burnaby, BC, Canada, August 14-16, 2013, Revised Selected Papers. pp. 265–285 (2013), http://dx.doi.org/10.1007/978-3-662-43414-7_14
20. Mangard, S., Oswald, E., Popp, T.: Power Analysis Attacks: Revealing the Secrets of Smart Cards (Advances in Information Security) (2007)
21. Masked WB-AES CASE1 sample binary.: https://github.com/SideChannelMarvels/Deadpool/tree/master/wbs_aes_lee_case1
22. Messerges, T.S.: Securing the AES Finalists Against Power Analysis Attacks. In: Fast Software Encryption, 7th International Workshop, FSE 2000, New York, NY, USA, April 10-12, 2000, Proceedings. pp. 150–164 (2000), http://dx.doi.org/10.1007/3-540-44706-7_11
23. Michiels, W., Gorissen, P., Hollmann, H.D.L.: Cryptanalysis of a Generic Class of White-Box Implementations. In: Selected Areas in Cryptography, 15th International Workshop, SAC 2008, Sackville, New Brunswick, Canada, August 14-15, Revised Selected Papers. pp. 414–428 (2008), http://dx.doi.org/10.1007/978-3-642-04159-4_27
24. Mulder, Y.D., Wyseur, B., Preneel, B.: Cryptanalysis of a Perturbated White-Box AES Implementation. In: Progress in Cryptology - INDOCRYPT 2010 - 11th International Conference on Cryptology in India, Hyderabad, India, December 12-15, 2010. Proceedings. pp. 292–310 (2010), http://dx.doi.org/10.1007/978-3-642-17401-8_21
25. Rivain, M., Wang, J.: Analysis and Improvement of Differential Computation Attacks against Internally-Encoded White-Box Implementations. IACR Trans. Cryptogr. Hardw. Embed. Syst. 2019(2), 225–255 (2019), <https://doi.org/10.13154/tches.v2019.i2.225-255>
26. Sasdrich, P., Moradi, A., Güneysu, T.: White-Box Cryptography in the Gray Box - - A Hardware Implementation and its Side Channels -. In: Fast Software Encryption - 23rd International Conference, FSE 2016, Bochum, Germany, March 20-23, 2016, Revised Selected Papers. pp. 185–203 (2016), http://dx.doi.org/10.1007/978-3-662-52993-5_10

27. Wyseur, B., Michiels, W., Gorissen, P., Preneel, B.: Cryptanalysis of White-Box DES Implementations with Arbitrary External Encodings. In: Selected Areas in Cryptography, 14th International Workshop, SAC 2007, Ottawa, Canada, August 16-17, 2007, Revised Selected Papers. pp. 264–277 (2007), http://dx.doi.org/10.1007/978-3-540-77360-3_17
28. Zeyad, M., Maghrebi, H., Alessio, D., Batteux, B.: Another Look on Bucketing Attack to Defeat White-Box Implementations. In: Constructive Side-Channel Analysis and Secure Design - 10th International Workshop, COSADE 2019, Darmstadt, Germany, April 3-5, 2019, Proceedings. pp. 99–117 (2019), https://doi.org/10.1007/978-3-030-16350-1_7